PRAMANA
— journal of
physics

Vol. 83, No. 5
November 2014
pp. 829–838

Neutrino and dark matter physics with sub-keV germanium detectors

ARUN KUMAR SOMA[1,2], LAKHWINDER SINGH[1,2], MANOJ KUMAR SINGH[1,2], VENKTESH SINGH[1,2] and HENRY T WONG[1,*], on behalf of the TEXONO Collaboration

[1]Institute of Physics, Academia Sinica, Taipei 11529, Taiwan
[2]Department of Physics, Banaras Hindu University, Varanasi 221 005, India
*Corresponding author. E-mail: htwong@phys.sinica.edu.tw

DOI: 10.1007/s12043-014-0876-5; ***e*Publication:** 4 November 2014

Abstract. Germanium detectors with sub-keV sensitivities open a window to study neutrino physics to search for light weakly interacting massive particle (WIMP) dark matter. We summarize the recent results on spin-independent couplings of light WIMPs from the TEXONO experiment at the Kuo-Sheng Reactor Neutrino Laboratory. Highlights of the physics motivation, our R&D programme, as well as the status and plans are presented.

Keywords. Neutrino interactions; dark matter; radiation detector.

PACS Nos 13.15.+g; 95.35.+d; 29.40.−n

1. Introduction

The current themes of the Taiwan-based Taiwan EXperiment On NeutrinO (TEXONO) and China-based China Dark matter EXperiment (CDEX) research programmes are on the studies of low-energy neutrino and dark matter physics. The current objectives are to open the 'sub-keV' detector window with germanium detectors [1]. The generic 'benchmark' goals in terms of detector performance are: (1) modular target mass of order of 1 kg, (2) detector sensitivities reaching the range of 100 eV and (3) background at the range of 1 kg^{-1} keV^{-1} day^{-1} (cpkkd). The neutrino physics programme [2,3] is pursued at the established Kuo-Sheng Reactor Neutrino Laboratory (KSNL), while dark matter searches are conducted at the new China Jinping Underground Laboratory (CJPL) [4,6] officially inaugurated in December 2010. The three main scientific subjects for research are neutrino magnetic moments [2,5], neutrino-nucleus coherent scattering [1] and dark matter searches [7].

We highlight the physics motivations, as well as the latest TEXONO results of the dark matter programme at KSNL in this paper.

2. Low-energy reactor neutrino physics

The observable spectra due to neutrino interactions on Ge target with reactor $\bar{\nu}_e$ at $\phi(\bar{\nu}_e) = 10^{13}$ cm^{-2} s^{-1} are depicted in figure 1.

Neutrino magnetic moment (μ_ν) is an intrinsic neutrino property which describes the possible neutrino–photon couplings in which the neutrino helicity is flipped [2,5]. Observations of μ_ν at levels relevant to the present or future generations of experiments which strongly favour the neutrinos are Majorana particles [8]. The μ_ν-induced neutrino–electron scattering $\bar{\nu}_e + e \rightarrow \bar{\nu}_e + e$ has a $1/T$ dependence modified by atomic binding energy effects [9], where T is the electron recoil energy. Accordingly, sensitivities will be enhanced to the $\sim 10^{-11}\mu_B$ level at 100 eV threshold.

Neutrino nucleus coherent scattering (νN): $\bar{\nu}_e + N \rightarrow \bar{\nu}_e + N$ is a fundamental neutrino interaction which has never been observed. In addition to the experiment with reactor neutrinos [1], projects with neutrinos from spallation neutron source [10] and accelerator [11] are also pursued. Measurement of the νN coherent scattering will provide a sensitive test to the Standard Model. The coherent interaction plays an important role in astrophysical processes. It may provide new approaches to the detection of supernova neutrinos and is a promising avenue towards a compact and relatively transportable neutrino detector for real-time monitoring of nuclear reactors.

After quenching effects are taken into account, the maximum measureable energy for nuclear recoil events in Ge due to reactor $\bar{\nu}_e$ is about 400 eV. The typical spectrum is depicted in figure 1. At benchmark sensitivities, the typical event rate is 10–20 kg^{-1} day^{-1} or 4000–7000 kg^{-1} yr^{-1} with a signal-to-background ratio >20. Low detector threshold is crucial in such experiments.

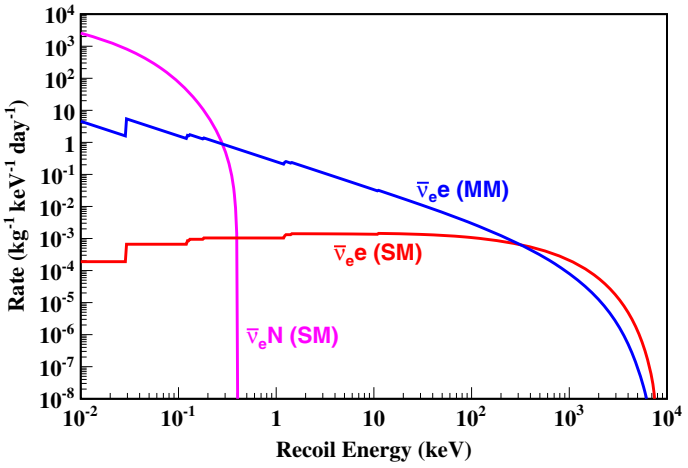

Figure 1. The observable spectra due to neutrino interactions on Ge target with reactor $\bar{\nu}_e$ at $\phi(\bar{\nu}_e) = 10^{13}$ cm^{-2} s^{-1}. Contributions due to magnetic moment-induced $\bar{\nu}_e$–e (MM) at $\mu_\nu = 10^{-10}\mu_B$, as well as Standard Model (SM) induced $\bar{\nu}_e$–e and $\bar{\nu}_e$–N coherent scattering are shown.

3. Light WIMP dark matter searches

There are compelling evidences that about one-quarter of the energy density in the Universe is composed of cold dark matter [7] due to a not-yet-identified particle, generically categorized as weakly interacting massive particle (WIMP, denoted by χ). A direct experimental detection of WIMP is one of the biggest challenges in the frontiers of particle physics and cosmology. The WIMPs interact with matter predominantly via elastic coherent scattering like neutrinos: $\chi + N \rightarrow \chi + N$. There may be both spin-independent ($\sigma^{\rm SI}_{\chi N}$) and spin-dependent ($\sigma^{\rm SD}_{\chi N}$) interactions between the WIMP and the matter.

An experiment with 100 eV threshold would open a window for cold dark matter WIMP searches in the unexplored mass range down to several GeV [1,6]. Based on the data taken at KSNL with the 20-g prototype ultra-low-energy germanium detector (ULEGe) and 900-g point contact germanium detector (PCGe), limits were derived in the low WIMP mass region, which showed an improvement over those from the previous experiments at $3 < m_\chi < 8$ GeV [12]. There are allowed regions implied by data from the DAMA/LIBRA, CoGeNT, CRESST-II and CDMS(Si) experiments [7,13]. These have stimulated intense theoretical interests and speculations on this parameter space.

The KSNL was originally built for reactor neutrino physics, where studies of neutrino magnetic moments and neutrino–electron scattering cross-sections [2,3] have been pursued. The CJPL [4,6] is the deepest operating underground laboratory in the world, having ∼2400 m of rock overburden and tunnel drive-in access. It is located at southwest Sichuan, China. The baseline design of the TEXONO experiment at KSNL and the CDEX-1 experiment at CJPL is depicted in figure 2. The germanium targets are enclosed

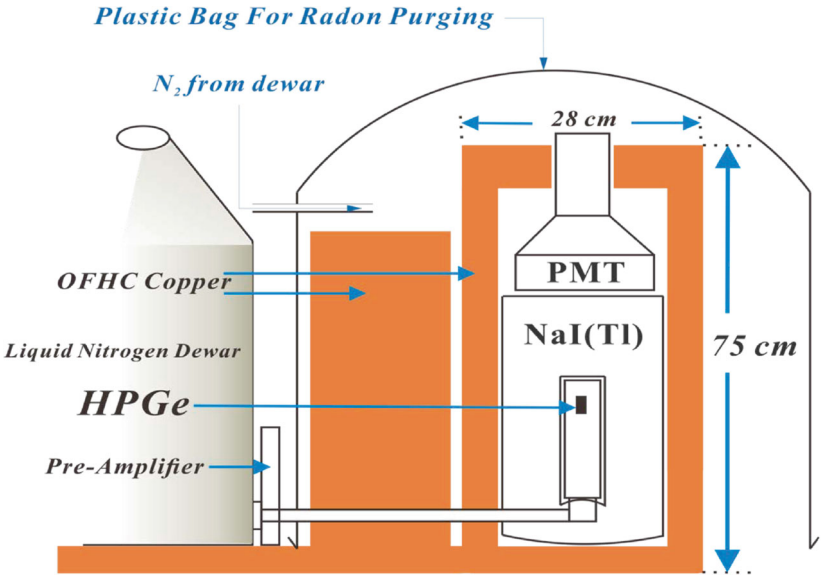

Figure 2. Baseline design with Ge target and NaI(Tl) crystal scintillator as anti-Compton detector, at both KSNL and CJPL.

by the active anti-Compton detector made of NaI(Tl) scintillating crystals, further surrounded by passive shielding of copper and a radon purge system. The entire system is enclosed inside shielding structures made of copper, boron-loaded polyethylene and lead. There is an additional cosmic-ray veto system with plastic scintillators at KSNL.

In addition, design and construction of the next-generation point-contact germanium detectors (PCGe) array with total mass at the 10 kg range is proceeding at CJPL. This new detector 'CDEX-10' will be shielded and enclosed in a liquid argon chamber which serves as both cryogenic medium and active shielding and anti-Compton detector where the scintillation light will be read out by photomultipliers.

4. Sub-keV germanium detectors

Point-contact germanium detectors (PCGe) [14] offer sub-keV sensitivities with detector having kg-size modular mass, an improvement over the conventional ULEGe design. WIMPs with mass down to a few GeV can be probed. Several R&D directions [6] are intensely pursued towards improvement on the threshold and background for sub-keV germanium detectors, some of them are:

(1) *Pulse shape analysis near noise-edge*
It has been demonstrated that by studying the correlation of the Ge signals in two different shaping times [12] as depicted in figure 3, the threshold can be further reduced below the hardware noise edge via pulse shape discrimination (PSD). The achieved thresholds at 50% signal efficiency are 220 and 310 eV for 20-g ULEGe and 500-g PCGe, respectively. The relative timing between the PCGe and anti-Compton (AC) NaI(Tl) detectors are shown in figure 4a, for 'sub-noise

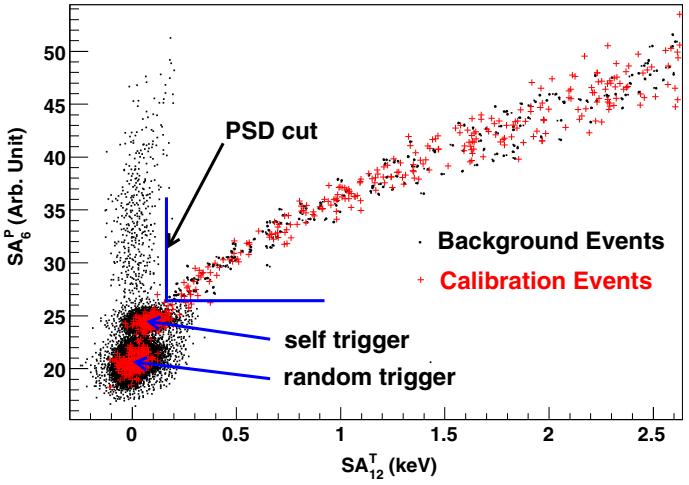

Figure 3. Scattered plots of the SA_6^P (shaping time is 6 μs with partial integration) vs. SA_{12}^T (shaping time is 12 μs with partial integration) signals, for both calibration and physics events. The PSD selection is shown.

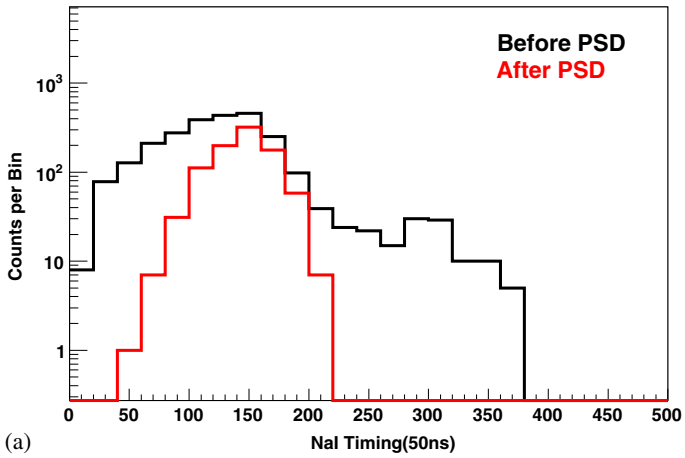

(a)

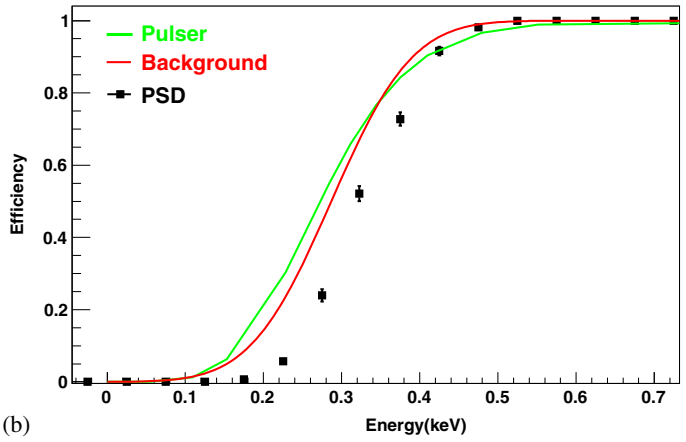

(b)

Figure 4. (**a**) Relative timing between AC-NaI(Tl) and PCGe systems, before and after PSD selection. The '50−200 ns' is the coincidence window where the signals at PCGe are mainly due to physics events correlated with the AC detector. (**b**) PSD selection efficiencies were derived from the survival probabilities of AC-tagged events. The trigger efficiencies of the 500-g PCGe detector, as derived from the test pulser and *in-situ* background events.

edge' events at 200–400 eV before and after PSD. Events in coincidence with AC at the '50−200 ns' window are due to multiple Compton scatterings, which are actual physical processes having similar pulse shapes as the neutrino and WIMP signals. The PSD selection efficiencies depicted in figure 4b were derived from the survival probabilities of the AC-tagged samples in the coincidence window. The trigger efficiencies were measured using two methods: the fractions of calibrated pulser events above the discriminator threshold provided the first measurement, while the studies on the amplitude distributions of *in-situ* background provided the other measurement.

(2) *Pulse shape analysis for surface vs. bulk events discrimination*
The surface events from p-type PCGe detectors exhibit anomalous behaviour due to incomplete charge collection. They can be differentiated from the signal bulk events because of their slower rise-time [6,15]. The rise-time distribution as well as the typical events are illustrated in figure 5a. Calibration schemes have been devised [15,16] using low- and high-energy γ-sources as well as an n-type PCGe detector where anomalous surface effects are absent. The measured

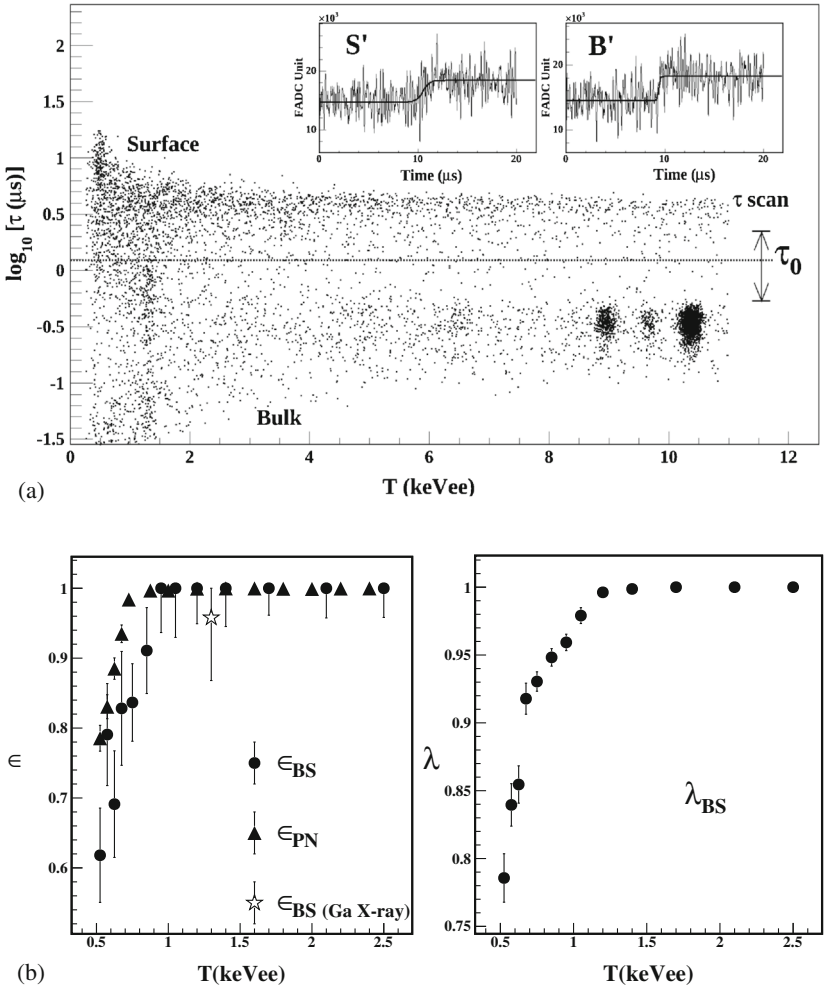

Figure 5. (**a**) Rise-time plots, as characterized by the amplitude of the fast timing amplifier signals, showing different behaviour between surface (faster) and bulk (slower) events. (**b**) The signal-retaining and background-suppression efficiencies (ϵ_{BS}, λ_{BS}) from the bulk-surface selection.

signal-retaining and background-suppression efficiencies ($\epsilon_{BS}, \lambda_{BS}$) are displayed in figure 5b.

(3) *Background understanding and suppression*
The MeV-range background was understood to the percent level in our previous neutrino–electron measurement with CsI(Tl) scintillating crystal array [3]. However, the residual spectra at KSNL [12,16] at the sub-keV energy range cannot be completely accounted for by conventional background modelling. Intense efforts on hardware cross-checks, further simulation and software analysis are underway. Data collection at CJPL, where the cosmic-induced background is absent, will also elucidate the origin of the observed sub-keV events.

(4) *Fabrication of advanced electronics for Ge detectors*
R&D programme is being pursued to produce advanced junction field-effect transistor (JFET) and pre-amplifier electronics with goals of further reducing the threshold and improving energy resolution. Data acquisition and trigger systems with real-time analysis capabilities using field programmable gate arrays (FPGA) are being installed.

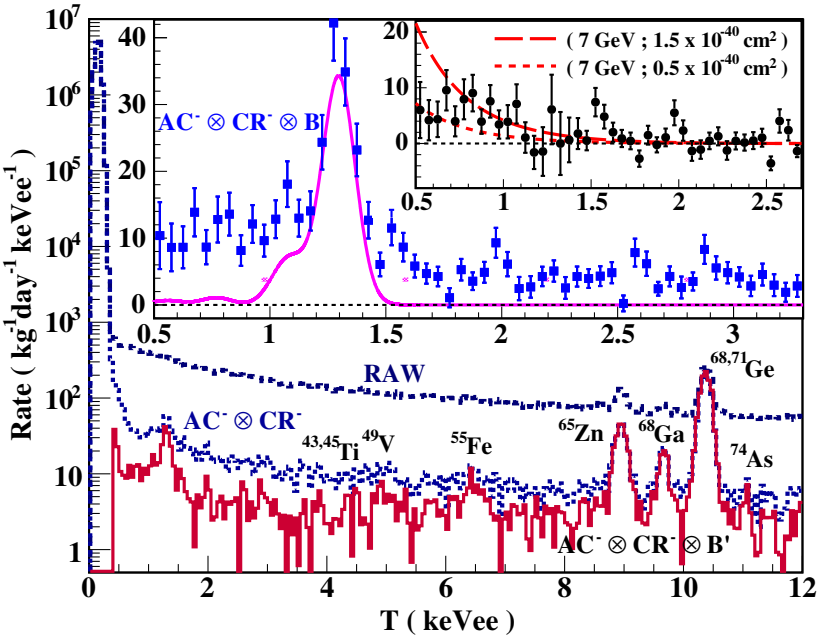

Figure 6. Measured energy spectra, showing the raw data and those with $AC^- \otimes CR^- (\otimes B')$ selections. The large inset shows the $(\epsilon_{BS}, \lambda_{BS})$-corrected $AC^- \otimes CR^- \otimes B$ spectrum, with a flat background and L-shell X-ray peaks overlaid. The small inset depicts the residual spectrum superimposed with that due to the allowed (excluded) cross-section at $m_\chi = 7$ GeV.

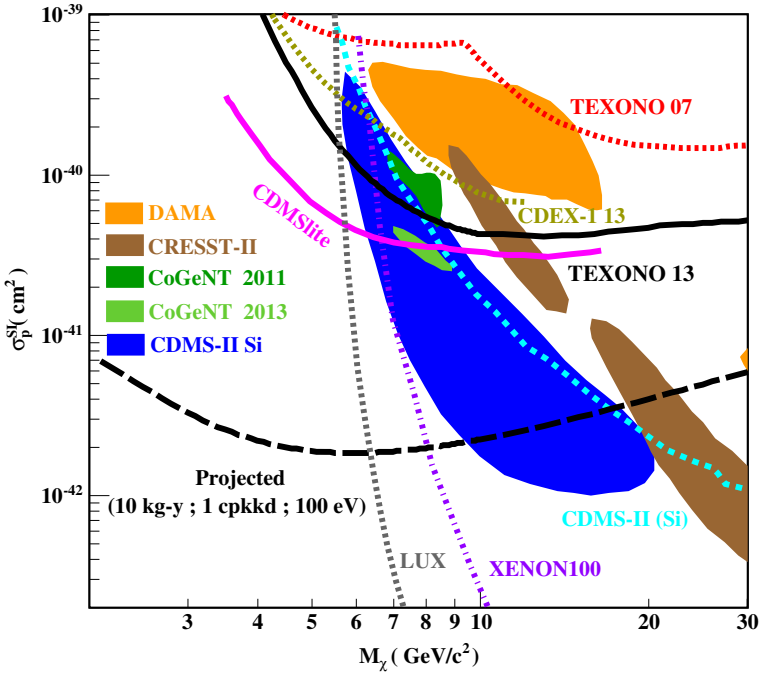

Figure 7. Exclusion plot of spin-independent χN cross-sections vs. WIMP-mass, displaying the TEXONO results [12,16] and those defining the current boundaries [7,17,18]. The allowed regions from the DAMA, CoGeNT, CRESST-II and CDMS(Si) experiments [7,13,19] are also shown. Projected reach of sub-keV Ge experiments at benchmark sensitivities are indicated as dotted lines.

5. Recent TEXONO results on spin-independent cross-sections

A total of 39.5 kg-days of data taken with a p-type PCGe detector at KSNL was analysed [16]. The application of cosmic-ray (CR) and NaI(Tl) anti-Compton (AC) vetos would lead to the $\mathrm{AC}^- \otimes \mathrm{CR}^-$ spectrum, with both detectors in anticoincidence. The selected events at various stages of the analysis are depicted in figure 6. The RAW spectrum above the electronic noise edge of 400 keV is due to physical events. Selection of bulk events according to figure 5a produce the measured $\mathrm{AC}^- \otimes \mathrm{CR}^- \otimes \mathrm{B}'$ spectrum, while the $(\epsilon_{\mathrm{BS}}, \lambda_{\mathrm{BS}})$-corrected spectrum for physics analysis is denoted as $\mathrm{AC}^- \otimes \mathrm{CR}^- \otimes \mathrm{B}$ in the large inset.

When the flat background due to high-energy γ-rays from ambient radioactivity and the contributions of L-shell X-rays are subtracted, the residual spectrum in the small inset of figure 6 can be interpreted as WIMP χN candidate events. The corresponding exclusion plot is displayed in figure 7, together with the results defining the sensitivity boundary in the light WIMP regions [7,17,18]. Part of the allowed regions of the DAMA, CoGeNT-2011(2014), CRESST-II and CDMS(Si) experiments [7,13,19] is probed and excluded.

6. Prospects and outlook

A detector with 1 kg modular mass, 100 eV threshold and 1 kg^{-1} keV^{-1} day^{-1} background level has important applications in neutrino and dark matter physics, as well as in the monitoring of reactor operation. Crucial advances have been made in adapting the Ge detector technology towards these requirements. Relevant limits have been achieved at KSNL on the WIMP couplings with matter. The sub-keV events are still to be understood. Intensive research programmes are being pursued along various fronts towards the realization of experiments which can meet all the technical challenges.

Further improvement in sensitivities can be expected with the 1-kg scale PCGe detectors already operating at KSNL and CJPL. The CDEX-1 results from CJPL were reported [20] and the exclusion curve is displayed in figure 7. Electronics will be improved and lower physics threshold can be expected. In addition, n-type PCGe detectors allow less ambiguous interpretation of the low-energy signals due to the absence of anomalous surface events. The next-generation CDEX-10 programme of 10-kg range PCGe enclosed in active liquid argon is being pursued.

Acknowledgements

The TEXONO Collaboration consists of groups from Taiwan (Academia Sinica, Kuo-Sheng Nuclear Power Station), China (Tsinghua University, Institute of Atomic Energy, Nankai University, Sichuan University), India (Banaras Hindu University) and Turkey (Middle East Technical University, Dokuz Eylül University). The authors are grateful to their contributions.

References

[1] Q Yue *et al*, *High Energy Phys. Nucl. Phys.* **28**, 877 (2004)
H T Wong *et al*, *J. Phys. Conf. Ser.* **39**, 266 (2006)
H T Wong *et al*, *J. Phys. Conf. Ser.* **120**, 042013 (2008)

[2] H B Li *et al*, *Phys. Rev. Lett.* **90**, 131802 (2003)
B Xin *et al*, *Phys. Rev. D* **72**, 012006 (2005)
H T Wong *et al*, *Phys. Rev. D* **75**, 012001 (2007)

[3] H B Li *et al*, *Nucl. Instrum. Methods A* **459**, 93 (2001)
Y Liu *et al*, *Nucl. Instrum. Methods A* **482**, 125 (2002)
Y F Zhu *et al*, *Nucl. Instrum. Methods A* **557**, 490 (2006)
M Deniz *et al*, *Phys. Rev. D* **81**, 072001 (2010)

[4] K J Kang *et al*, *J. Phys. Conf. Ser.* **203**, 012028 (2010)
D Normile, *Science* **324**, 1246 (2009)
K J Kang *et al*, *Front. Phys. China* **8**, 412 (2013)

[5] H T Wong and H B Li, *Mod. Phys. Lett. A* **20**, 1103 (2005) and references therein

[6] H T Wong, *Int. J. Mod. Phys. D* **20**, 1463 (2011)
Q Yue and H T Wong, *Mod. Phys. Lett. A* **28**, 1340007 (2013)

[7] Particle Data Group: J Beringer *et al*, *Phys. Rev. D* **86**, 010001, 289 (2012) and references therein

[8] S Davidson, M Gorbahn and A Santamaria, *Phys. Lett. B* **626**, 151 (2005)
N F Bell *et al*, *Phys. Rev. Lett.* **95**, 151802 (2005)
N F Bell *et al*, *Phys. Lett. B* **642**, 377 (2006)
[9] V I Kopeikin *et al*, *Phys. Atom. Nucl.* **60**, 2032 (1997)
S A Fayans, L A Mikaelyan and V V Sinev, *Phys. Atom. Nucl.* **64**, 1475 (2001)
K A Kouzakov, A I Studenikin and M B Voloshin, *Phys. Rev. D* **83**, 113001 (2011)
J W Chen *et al*, arXiv:1311.5294 (2013)
[10] D Akimov *et al*, arXiv:1310.0125 (2013) and references therein
[11] S J Brice *et al*, arXiv:1311.5958 (2013) and references therein
[12] H T Wong, *Mod. Phys. Lett. A* **23**, 1431 (2008)
S T Lin *et al*, *Phys. Rev. D* **76**, 061101(R) (2009)
[13] C E Aalseth *et al*, *Phys. Rev. Lett.* **106**, 131301 (2011); *Phys. Rev. Lett.* **107**, 141301 (2011); *Phys. Rev. D* **88**, 012002 (2013); arXiv:1401.3295 (2014)
[14] P N Luke *et al*, *IEEE Trans. Nucl. Sci.* **36**, 926 (1989)
P A Barbeau, J I Collar and O Tench, *J. Cosmol. Astropart. Phys.* **09**, 009 (2007)
[15] H B Li *et al*, *Astropart. Phys.*, in press (2014) arXiv:1311.5957
[16] H B Li *et al*, *Phys. Rev. Lett.* **110**, 261301 (2013)
[17] R Agnese, *Phys. Rev. Lett.* **112**, 041302 (2014)
[18] D S Acre, *Nucl. Instrum. Methods A* **704**, 111 (2013)
D S Akerib, arXiv:1310.8214 (2013)
[19] R Agnese, *Phys. Rev. Lett.* **111**, 251301 (2013)
R Agnese, *Phys. Rev. D* **88**, 031104 (2013)
[20] W Zhao *et al*, *Phys. Rev. D* **88**, 052004 (2013)
K J Kang *et al*, *Chin. Phys. C* **37**, 126002 (2013)